Unrestrained Molecular Dynamics Simulations of $[d(AT)_5]_2$ Duplex in Aqueous Solution: Hydration and Binding of Sodium Ions in the Minor Groove

Richard Štefl[†,‡] and Jaroslav Koča*[,†,§]

Laboratory of Biomolecular Structure and Dynamics, Department of Theoretical and Physical Chemistry, and Department of Organic Chemistry, Masaryk University, Kotlářská 2, CZ-611 37 Brno, Czech Republic

Received April 16, 1999. Revised Manuscript Received January 26, 2000

Abstract: The results of unrestrained particle mesh Ewald molecular dynamics simulations of the $[d(AT)_5]_2$ duplex in aqueous solution are presented here. Two trajectories starting from A (10 ns) and B (5 ns) canonical forms were carried out. Both trajectories converged within about 500 ps and produced stable and similar conformational ensembles, which exhibit the qualitative features of B-DNA. Surprisingly, the convergence of hydration patterns is much slower than the convergence of the solute structure. We observed intrusions of sodium ions into the minor groove of the ApT steps with residence times of about 1−2 ns. The sodium ions were coordinated by the electronegative potential of O2 atoms of thymines, which induce a large negative propeller twist. The propeller twist change is related to the repulsion between a sodium ion and H2 atoms of adenines in the minor groove. It simultaneously leads to rather close mutual amino group contacts of adenine amino groups in ApT steps frequently occurring in nucleotide crystals. We have suggested a relationship between the coordination of sodium ions at the ApT steps and the close approach of the adenine amino groups in the same step.

Introduction

It has already been shown by Franklin and Gosling[1] that as the humidity of the DNA sample increased, the characteristics of the fiber diffraction pattern changed. The early crystal structure determinations of dinucleoside phosphates[2−4] demonstrated the presence of ordered water in crystals and led to the concept of water involvement in the recognition process.[5] However, it was the observation of the spine of hydration in the first B-DNA crystal structure[6] that made it necessary to consider seriously the concept of water as an integral part of nucleic acids.[7] The spine of hydration first seen in the crystal structure of the B-DNA dodecamer duplex d(CGCGAATTCGCG)[8,9] was composed of two layers of water molecules, and it was postulated that it was specific to AT tracts, where the N3 atom of adenine and the O2 atom of thymine are readily available as hydrogen bond acceptors in interactions with water molecules.[6] The spine was also observed in many other crystal structures of B-DNA.[10−13] What had been observed in the B-DNA crystal structures using X-ray crystallography, was also confirmed in solution by NMR spectroscopy.[14−16] Unlike Drew-Dickerson's original description of the spine, which considers two layers of water molecules, recently reported high-resolution crystal structures of the d(CGCGAATTCGCG) indicate that the spine is four layers deep and combines to form a repeating motif of fused hexagons.[17−19] Thus, the highly ordered molecules of the solvent are not only connected with the possible stabilizing effect of a solvent on B-DNA, but they also represent a way in which the DNA sequence information could be transmitted into solvent regions, which may have far-reaching consequences for the recognition processes.

Recently, several studies about the solvation status of the minor groove of the B-DNA have been reported. In particular,

* Author for correspondence. Telephone: +420-5-41129310. Fax: +420-5-41129506. E-mail: jkoca@chemi.muni.cz.
† Laboratory of Biomolecular Structure and Dynamics.
‡ Department of Theoretical and Physical Chemistry.
§ Department of Organic Chemistry.

(1) Franklin, R. E.; Gosling, R. G. *Nature* **1953**, *171*, 740.
(2) Rosenberg, J. M.; Seeman, N. C.; Kim, J. J.; Suddath, F. L.; Nicholas, H. B.; Rich, A. *Nature* **1973**, *243*, 150−154.
(3) Rosenberg, J. M.; Seeman, N. C.; Day, R. O.; Rich, A. *J. Mol. Biol.* **1976**, *104*, 145−167.
(4) Seeman, N. C.; Rosenberg, J. M.; Suddath, F. L.; Kim, J. J.; Rich, A. *J. Mol. Biol.* **1976**, *104*, 109−144.
(5) Seeman, N. C.; Rosenberg, J. M.; Rich, A. *Proc. Natl. Acad. Sci. U.S.A.* **1976**, *73*, 804.
(6) Drew, H. R.; Dickerson, R. E. *J. Mol. Biol.* **1981**, *151*, 535−556.
(7) Berman, H. M.; Schneider, B. In *Oxford handbook of nucleic acid structure*; Neidle, S., Ed.; Oxford University Press: New York, 1999; pp 295−310.
(8) Drew, H. R.; Wing, R. M.; Takano, T.; Broka, C.; Tanaka, S.; Itakura, K.; Dickerson, R. E. *Proc. Natl. Acad. Sci. U.S.A.* **1981**, *78*, 2179−2183.
(9) Dickerson, R. E.; Drew, H. R. *J. Mol. Biol.* **1981**, *149*, 761−786.
(10) Berman, H. M.; Olson, W. K.; Beveridge, D. L.; Westbrook, J.; Gelbin, A.; Demeny, T.; Hsieh, S. H.; Srinivasan, A. R.; Schneider, B. *Biophys. J.* **1992**, *63*, 751−759.
(11) Schneider, B.; Cohen, D.; Berman, H. M. *Biopolymers* **1992**, *32*, 725−750.
(12) Shatzky-Schwartz, M.; Arbuckle, N. D.; Eisenstein, M.; Rabinovich, D.; Bareket-Samish, A.; Haran, T. E.; Luisi, B. F.; Shakked, Z. *J. Mol. Biol.* **1997**, *267*, 595−623.
(13) Shui, X.; McFail-Isom, L.; Hu, G. G.; Williams, L. D. *Biochemistry* **1998**, *37*, 8341−8355.
(14) Liepinsh, E.; Otting, G.; Wuthrich, K. *Nucleic Acids Res.* **1992**, *20*, 6549−6553.
(15) Kubinec, M. G.; Wemmer, D. E. *J. Am. Chem. Soc.* **1992**, *114*, 8739−8740.
(16) Denisov, V. P.; Carlstrom, G.; Venu, K.; Halle, B. *J. Mol. Biol.* **1997**, *268*, 118−136.
(17) Shui, X. Q.; Sines, C. C.; McFail-Isom, L.; VanDerveer, D.; Williams, L. D. *Biochemistry* **1998**, *37*, 16877−16887.
(18) Tereshko, V.; Minasov, G.; Egli, M. *J. Am. Chem. Soc.* **1999**, *121*, 470−471.
(19) Tereshko, V.; Minasov, G.; Egli, M. *J. Am. Chem. Soc.* **1999**, *121*, 3590−3595.

10.1021/ja9912170 CCC: $19.00
Published on Web 05/12/2000

the specific binding of monovalent ions in the minor groove was studied using X-ray crystallography,[13,17,19] NMR spectroscopy,[20] and theoretical methods.[21,22] The X-ray crystal structure of d(CGCGAATTCGCG) dodecamer (at a resolution of 1.4 Å) suggested that the primary spine is partially occupied by sodium ions,[13] while the other crystal structures of d(CGCGAATTCGCG) dodecamer (at a resolution of 1.1 Å) and d(GCGAATTCG) nonamer (at a resolution of 0.9 Å), showed no evidence for the presence of sodium ions in the minor groove.[18,23] It should be noted that the crystals were grown using high concentrations of Mg^{2+} in order to achieve better diffraction. However, the high concentration of divalent cations may have an impact on the DNA structure. Specifically, the high concentration of Mg^{2+} may expel sodium ions from the minor groove. Shui et al. reported an X-ray experiment where potassium substitution for sodium confirmed that monovalent cations penetrate the primary layer of the spine of hydration.[17] The authors also suggested that some solvent sites traditionally thought to be water molecules are in fact partially occupied by water molecules and monovalent cations. The use of an isotopically labeled ammonium ion as a probe in high-resolution NMR spectroscopy allows the monovalent cation binding sites on the DNA duplex in solution to be localized. This technique revealed a preference for the binding of ammonium cations in the minor groove of A-tract sequences.[20] A theoretical approach based mainly on molecular dynamics (MD) simulations showed the intrusion of the sodium ion into the spine of hydration in the minor groove of the B-DNA dodecamer d(CGCGAATTCGCG).[21] The sodium ion was found to be localized at the ApT step in the minor groove (with a residence time of about 500 ps). The authors termed this position the "ApT pocket".[21] This site was previously noted to be of uniquely low negative electrostatic potential relative to that of other positions in the groove.[24] These findings are also supported by the location of a sodium ion in the crystal structure of the dinucleoside phosphates (dApU), where a sodium ion was coordinated with the two cross-strand uridine O2 oxygens.[4]

Briefly, the "spine of hydration" has been well-established by X-ray crystallography, confirmed by NMR spectroscopy, and also reproduced by MD. However, the problem of sodium ions binding in the minor groove is still not entirely clear and it is a matter of controversy in the literature. While NMR spectroscopy and theoretical approaches clearly suggest the sites where the sodium ions may be coordinated, X-ray crystallography cannot answer this question so surely. The resolution of the B-DNA structures makes it difficult to distinguish sodium ions from water molecules, especially if the occupancy of the sodium ions is less than 50%. The problem is that sodium ions and water molecules contain the same number of electrons (giving electron density peaks with similar volumes and having pliable and unpredictable coordination geometries) and form solvation patterns for which the water occupancy is higher than the sodium occupancy.[17] Further X-ray experimental analyses at higher resolution are needed to resolve this issue.

Another remarkable structural feature of the ApT steps is the formation of close mutual adenine amino group contacts in the major groove. The average N6−N6 distance in the ApT steps in B-DNA crystal structures is around 3.15 Å. This is the closest and statistically most significant contact of exocyclic groups occurring in nucleic acids.[25] It has also been shown that these close amino group contacts are systematically lacking in those ApT steps having a true 2-fold symmetry.[26] It has been suggested that an attractive amino group interaction requires an asymmetric arrangement of two amino groups, where one of the two amino groups acts as a donor of a weak out-of-plane hydrogen bond while the other amino group serves as a H-bond acceptor. As revealed by ab initio quantum chemical calculations when 2-fold symmetry is imposed, the amino group interaction is purely repulsive.[26] There is currently an ongoing debate about what the physical origin of these experimental observations is.[27] An example of an amino-acceptor interaction has recently been found in a 1.9 Å resolution crystal structure of an unusual DNA−DAPI complex.[28]

The present contribution is concerned with the deoxynucleotide $[d(AT)_5]_2$, carrying the alternating sequence of adenines and thymines. Although the alternating sequences of adenines and thymines are very interesting from the point of view of hydration and the binding of ions, they have been studied less frequently than the AT sequences forming A-tracts. The alternating poly(dA-dT) sequences, which belong to the most flexible ones,[29] were found by NMR spectroscopy in a normal B-DNA conformation,[30,31] left-handed B-type conformation,[32] and wrinkled D-form conformation.[33] In addition, the following duplex shapes were suggested by X-ray diffraction studies for alternating poly(dA-dT): A-DNA,[34] B-DNA,[35] alternating B-DNA,[36] C-DNA,[37] right-handed D-DNA,[38] left-handed D-DNA with Hoogsteen base pairing,[39] and wrinkled D-DNA.[40] Extreme conformational variability of the alternating poly(dA-dT) is also supported by the observation of an additional type of duplex, called X-DNA.[41] The formation and stabilization of the various DNA shapes are strongly dependent upon the environment. Variations in ionic strength and identity, water activity, and ligand/protein binding are the main contributions, which together with the sequence can modulate DNA structure.

We have been concerned first with the question of how well we can reproduce the coordination of sodium ions and the close mutual amino group contacts observed in the ApT steps by applying ns-scale MD simulations and second with the question

(20) Hud, N. V.; Sklenář, V.; Feigon, J. *J. Mol. Biol.* **1999**, *286*, 651−660.
(21) Young, M. A.; Jayaram, B.; Beveridge, D. L. *J. Am. Chem. Soc.* **1997**, *119*, 59−69.
(22) Young, M. A.; Ravishanker, G.; Beveridge, D. L. *Biophys. J.* **1997**, *73*, 2313−2336.
(23) Soler-Lopez, M.; Malinina, L.; Liu, J.; Huynh-Dinh, T.; Subirana, J. A. *J. Biol. Chem.* **1999**, *274*, 23683−6.
(24) Lavery, R.; Pullman, B. *J. Biomol. Struct. Dyn.* **1985**, *2*, 1021−1032.
(25) Šponer, J.; Kypr, J. *Int. J. Biol. Macromol.* **1994**, *16*, 3−6.
(26) Šponer, J.; Hobza, P. *J. Am. Chem. Soc.* **1994**, *116*, 709−714.
(27) Luisi, B.; Orozco, M.; Šponer, J.; Luque, F. J.; Shakked, Z. *J. Mol. Biol.* **1998**, *279*, 1123−36.
(28) Vlieghe, D.; Šponer, J.; Meervelt, L. V. *Biochemistry* **1999**, *38*, 16443−16451.
(29) Chen, H. H.; Rau, D. C.; Charney, E. *J. Biomol. Struct. Dyn.* **1985**, *2*, 709−719.
(30) Assa-Munt, N.; Kearns, D. R. *Biochemistry* **1984**, *23*, 791−796.
(31) Borah, B.; Cohen, J. S.; Bax, A. *Biopolymers* **1985**, *24*, 747−765.
(32) Gupta, G.; Sarma, M. H.; Dhingra, M. M.; Sarma, R. H.; Rajagopalan, M.; Sasisekharan, V. *J. Biomol. Struct. Dyn.* **1983**, *1*, 395−416.
(33) Suzuki, E.; Pattabiraman, N.; Zon, G.; James, T. L. *Biochemistry* **1986**, *25*, 6854−6865.
(34) Davies, D. R.; Baldwin, R. L. *J. Mol. Biol.* **1963**, *6*, 251−255.
(35) Arnott, S.; Hukins, D. W. L. *Biochem. Biophys. Res. Commun.* **1972**, *47*, 1504−1509.
(36) Klug, A.; Jack, A.; Viswamitra, M. A.; Kennard, O.; Shakked, Z.; Steitz, T. A. *J. Mol. Biol.* **1979**, *131*, 669−680.
(37) Marvin, D. A.; Spencer, M.; Wilkins, M. H. F.; Hamilton, L. D. *J. Mol. Biol.* **1961**, *3*, 547−565.
(38) Arnott, S.; Selsing, E. *J. Mol. Biol.* **1974**, *88*, 509−521.
(39) Drew, H. R.; Dickerson, R. E. *EMBO J.* **1982**, *1*, 663−667.
(40) Arnott, S.; Chandrasekaran, R.; Puigjaner, L. C.; Walker, J. K.; Hall, I. H.; Birdsall, D. L.; Ratliff, R. L. *Nucleic Acids Res.* **1983**, *11*, 1457−1474.
(41) Kypr, J.; Vorlíčková, M. *Conformations of DNA duplexes containing (dA-dT) sequences of bases and their possible biological significance*; Sarma, R. H., Sarma, M. H., Eds.; Adenine Press: 1988; Vol. 2, pp 105−121.

of what are the dynamics related to these phenomena. On the basis of the present simulations, we suggest that sodium coordination and amino group contacts can in fact be interrelated and that they lead to the rather rigid geometry of the ApT steps observed in the crystal structures. This geometry is mainly characterized by a large propeller twist of the base pairs. Our suggestion is based on the results obtained by long MD simulations of the sequence containing a number of independent ApT steps. We believe we have a suitable model providing enough data to study the spine of hydration, the influence of the direct and indirect coordination of the sodium ions in the grooves, and the formation of the close mutual amino group contacts.

Methods and Simulation Protocols

The starting canonical A-[35] and B-shape[42] duplex structures of $[d(AT)_5]_2$ were generated using the NUCGEN module of AMBER 5.0.[43,44] The structures were neutralized by sodium ions initially placed using Coulombic potential terms with the LEaP module of AMBER 5.0 and then were surrounded by a periodic box of water molecules described by the TIP3P potential.[45,46] The water box was extended to a distance of 10 Å away from any solute atom. This yielded about 3300 and 3500 water molecules used for the solvation of the canonical A- and B-shape duplex structures of $[d(AT)_5]_2$, respectively. The all-atom force field parameters described by Cornell et al.[47] were used in all of the simulations. All of the calculations were carried out using the SANDER module of AMBER 5.0 with SHAKE[48] on the hydrogens with a tolerance of 5×10^{-4} Å, a 2 fs time step for the integration of the Newton's equations, a temperature of 300 K with Berendsen temperature coupling[49] with a time constant of 0.2 ps, a 9 Å cutoff applied to the Lennard-Jones interactions, and constant pressure of 1 atm. The nonbonded pair list was updated every 10 steps. Equilibration was started by 1000 steps minimization with the position of the DNA fixed. After this initial step of the equilibration protocol, all subsequent simulations were performed using the particle mesh Ewald[50] (PME) approach for evaluating long-range electrostatic effects. The PME charge grid spacing was approximately 1 Å, and the charge grid was interpolated using a cubic B-spline with the direct sum tolerance of 10^{-6} at the 9 Å direct space cutoff. The next steps of the equilibration protocol were: 25 ps of MD simulation with the position of the DNA fixed, 1000 steps of minimization with 25 kcal/(mol·Å^2) restraints placed on all solute atoms, 3 ps of MD simulation with 25 kcal/(mol·Å^2) restraints placed on all solute atoms, 5 rounds of 1000-steps minimization where the solute restraints were reduced by 5 kcal/(mol·Å^2) during each round. At the end of the equilibration protocol, 20 ps MD simulation was carried out, with the system heated from 100 to 300 K over 2 ps. In the course of our MD simulations, the coordinates were saved after each picosecond. All of the results were analyzed using CARNAL and RDPARM modules of AMBER 5.0 and the Dials and Windows[51] interface to Curves.[52] The Curves program, which fits the global axis through the base pairs, was used to determine the helicoidal parameters, defined previously.[53] Pseudorotation phase angles and amplitudes were calculated on the basis of the Altona and Sundaralingam convention.[54] Nucleic acid residue names are referred to in the text as one letter codes. Where necessary, a subscript for the residue number is also presented; the residue number is in the 5′-to-3′ direction with the first strand numbered 1−10 and the second strand 11−20. The last 1000 ps of each trajectory were used to obtain averaged structures. No extra processing of these averaged structures was performed except for the structure intended for the additional calculations. Here, the molecule was minimized using steepest descent and conjugate gradient techniques to remove the most serious geometrical artifacts introduced by the averaging procedure (e.g., bad C−H bond lengths in the methyl groups). To prevent this minimization from changing the structure too much, all heavy atoms were restrained to their initial positions with a force constant of 100 kcal/(mol·Å^2).

Calculations of electrostatic potential of $[d(AT)_5]_2$-counterion system (salt concentration 0.145 mol/dm^3) based on the nonlinear Poisson−Boltzmann equation were performed using the DELPHI program.[55,56] The Cornell et al. charges and van der Waals parameters were used.[47] Dielectric responses of 2 and 80 were assigned to the solute and water, respectively.

Ab initio calculations of electrostatic potential of the ApT and TpA pockets were performed using the TURBOMOLE[57] module interfaced with the INSIGHTII.[58] The density functional theory using the Becke 3LYP functional[59,60] with the 6-31G** basis set was used in all the ab initio calculations. Only four DNA bases (without sugar−phosphate backbone) were included in the calculations for each pocket.

All of the molecular graphics works presented here were produced using the UCSF MIDAS Plus[61] and InsightII[58] software. The calculations were carried out on SGI R10000 (Power Challenge and Origin 200) computers.

Results

Convergence of the d[(AT)$_5$]$_2$ Decamer. We have run two MD simulations. They started from the canonical A (10 ns) and B (5 ns) form of $[d(AT)_5]_2$ decamer, respectively. Both the starting structures converged during the MD simulations into a "common" structure, which exhibits qualitative characteristics of B-DNA. The convergence was evaluated by one-dimensional root-mean-square deviations (RMSD) from the canonical B-DNA (data not shown here) and occurred within about 500 ps in both simulations. This "common" structure was relatively conserved during the rest of the simulations exhibiting RMSD fluctuations ± 0.6 Å. RMSD was not the only criterion used to analyze the convergence of the MD trajectories. We have also included some helicoidal parameters in the analysis. The plots in Figure 1 clearly show A-to-B form transition at the time scale of 500 ps (dashed line) expressed in the helicoidal parameters. In this figure, *x*-displacement, inclination, rise, and pseudorotation phase angle averaged over all residues are plotted as a

(42) Arnott, S.; Hukins, D. W. L. *J. Mol. Biol.* **1973**, *81*, 93−105.
(43) Pearlman, D. A.; Case, D. A.; Caldwell, J. W.; Ross, W. S.; Cheatham, T. E., III; DeBolt, S.; Ferguson, D. M.; Seibel, G. L.; Kollman, P. A. *Comput. Phys. Commun.* **1995**, *91*, 1−41.
(44) Case, D. A.; Pearlman, D. A.; Caldwell, J. W.; Cheatham, T. E., III; Ross, W. S.; Simmerling, C. L.; Darden, T. A.; Merz, K. M.; Stanton, R. V.; Cheng, A. L.; Vincent, J. J.; Crowley, M.; Ferguson, D. M.; Radmer, R. J.; Seibel, G. L.; Singh, U. C.; Weiner, P. K.; Kollman, P. A. *AMBER* 5.0; University of California: San Francisco, 1997.
(45) Jorgensen, W. L.; Chandrasekhar, J.; Madura, J. D.; Impey, R. W.; Klein, M. L. *J. Chem. Phys.* **1983**, *79*, 926−935.
(46) Jorgensen, W. L. *J. Am. Chem. Soc.* **1981**, *103*, 341−345.
(47) Cornell, W. D.; Cieplak, P.; Bayly, C. I.; Gould, I. R.; Merz Jr., K. M.; Ferguson, D. M.; Spellmeyer, D. C.; Fox, T.; Caldwell, J. W.; Kollman, P. A. *J. Am. Chem. Soc.* **1995**, *117*, 5179−5197.
(48) Ryckaert, J. P.; Ciccotti, G.; Berendsen, H. J. C. *J. Comput. Phys.* **1977**, *23*, 327−341.
(49) Berendsen, H. J. C.; Postma, J. P. M.; van Gunsteren, W. F.; DiNola, A.; Haak, J. R. *J. Chem. Phys.* **1984**, *81*, 3684−3690.
(50) Essmann, U.; Perera, L.; Berkowitz, M. L.; Darden, T. A.; Lee, H.; Pedersen, L. G. *J. Chem. Phys.* **1995**, *103*, 8577−8593.
(51) Ravishanker, G.; Swaminathan, S.; Beveridge, D. L.; Lavery, R.; Sklenar, H. *J. Biomol. Struct. Dyn.* **1989**, *6*, 669−699.
(52) Lavery, R.; Sklenar, H. *J. Biomol. Struct. Dyn.* **1988**, *6*, 63−91.
(53) Dickerson, R. E. *J. Mol. Biol.* **1989**, *205*, 787−791.
(54) Altona, C.; Sundaralingam, M. *J. Am. Chem. Soc.* **1972**, *94*, 8205−8212.
(55) Gilson, M. K.; Sharp, K. A.; Honig, B. H. *J. Comput. Chem.* **1988**, *9*, 327−335.
(56) Sharp, K. A.; Nicholls, A. *DelPhi* 3.0; Columbia University: New York, 1989.
(57) Ahlrichs, R.; Bär, M.; Häser, M.; Horn, H.; Kölmel, C. *Chem. Phys. Lett.* **1989**, *162*, 165−169.
(58) INSIGHTII.; Biosym/MSI: San Diego, 1995.
(59) Becke, A. D. *J. Chem. Phys.* **1993**, *98*, 5648−5652.
(60) Lee, C.; Yang, W.; Parr, R. G. *Phys. Rev. B* **1988**, *37*, 785.
(61) Ferrin, T. E.; Huang, C. C.; Jarvis, L. E.; Langridge, R. *J. Mol. Graphics* **1988**, *6*, 13−27.

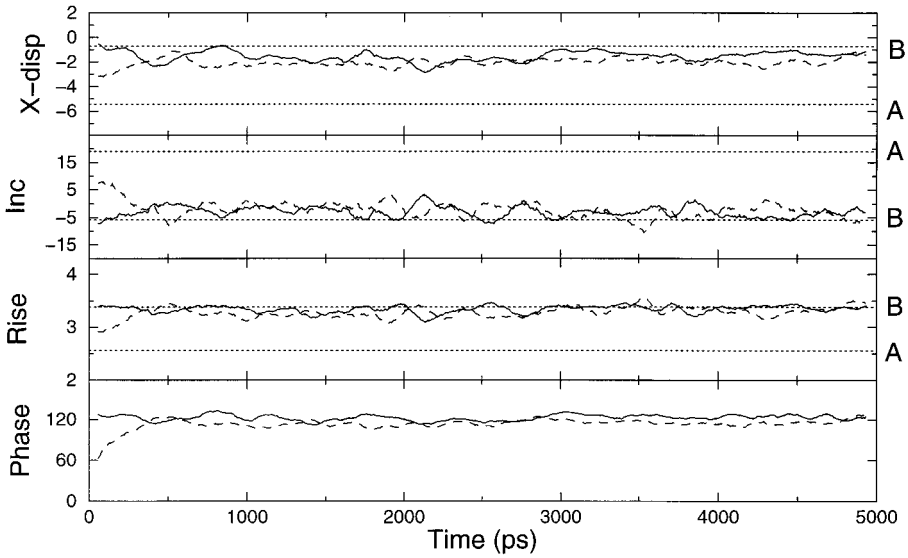

Figure 1. Several representative geometrical parameters (*x*-displacement (Å), Inclination (deg), rise (Å) and pseudorotation phase angle (deg)) calculated with the Dials and Windows[51] interface to Curves[52] for each the fifth frame of the simulation starting from the canonical B-form of the $[d(AT)_5]_2$ decamer (solid lines) and half of the simulation starting from the canonical A-form of the $[d(AT)_5]_2$ decamer (dashed lines) are shown as a function of time. The data have been smoothed by performing a running average in time over 50 ps. All of the geometrical parameters are averaged over all of the residues. For the helicoidal parameters, the canonical values are also plotted (dotted lines). For more details see the text.

function of time for both simulations. It is seen that after about 500 ps, the values of *x*-displacement, inclination, and rise become very close to the canonical B-DNA.

Convergence of the Oligonucleotide Hydration. Unlike the convergence of the $[d(AT)_5]_2$ decamer, which is transparent, the convergence of the hydration patterns is more complex. This is seen in Figures 2 and 3 which provide a general picture of the overall hydration and characterize the distinction between the hydration of the individual segments of the trajectories. Figure 2 shows the water oxygen atom density in different periods of the simulation starting from the canonical B-form of the $[d(AT)_5]_2$ decamer (contoured about 3.6-times the bulk water density and with the average oligonucleotide structures computed from the corresponding trajectory segments). Because of the transition from the canonical B-DNA during the first 500 ps, the hydration over the first nanosecond is weak (Figure 2a). In the course of the second nanosecond, the structure of the $[d(AT)_5]_2$ decamer becomes stable and, hence, a stable hydration pattern is formed (Figure 2b). This hydration pattern, the spine of hydration, is similar to that which has been reported for crystal structures.[6,10−13] The highest, and relatively constant, oxygen atom densities are observed over the third, fourth, and fifth (Figure 2c) nanoseconds. Here, the hydration pattern is stable and changes only slightly depending on the penetration of sodium ions into the minor groove. At the lower contour level (∼2.9-times the bulk water density (Figure 2d)), the overall hydration of the $[d(AT)_5]_2$ decamer (over the fifth nanosecond) is shown. In addition to the well-defined two layers of the spine of hydration (vide infra), the hydration of the major groove and the phosphate groups is visible. Figure 3 shows the water oxygen atom density for selected periods of the simulation starting from the canonical A-form of the $[d(AT)_5]_2$ decamer. Since the A-to-B transition occurs during the first 500 ps, the average structure of the $[d(AT)_5]_2$ decamer over the first nanosecond of this simulation is a hybrid of A- and B-forms and also the hydration pattern exhibits characteristics of both forms (Figure 3a,b). While the structure of the oligonucleotide is relatively stable after the initial A-to-B transition, the hydration patterns show residual A-form hydration until the eighth nanosecond (Figure 3c−f) is reached. The hydration pattern and its density after the eighth nanosecond corresponds to the hydration seen in the simulation starting from the canonical B-form after about 3 ns. This "convergence delay" will be addressed in the Discussion.

Note that the spine of hydration observed in our MD data is only two layers deep in contrast to the high-resolution crystallographic data which shows the spine of hydration as four layers deep and combining to form a repeating motif of fused hexagons. This is shown in Figure 4, where a part of the water oxygen atom density and the fused hexagons are shown.

The Overall Geometry of the Double Helix and of the ApT and TpA Steps. As mentioned above, after the convergence of the trajectories, the overall geometry exhibits features of the B-DNA family. The typical central hole characterizing A-DNA when viewed end-on is not seen in the resulting double helix. The helix contains B-type puckering of the deoxyribose rings, and its helicoidal parameters fall into the B-family of DNA, for example, rise 3.3 Å, *x*-displacement −1.9 Å, inclination 2.0° (calculated with respect to the global helical axis).

The alternating AT sequence is composed of two steps (ApT and TpA) which have completely different stacking as seen in Figure 5. The stacking of ApT and TpA steps in our simulations is very similar to the stacking of these steps obtained from the analysis of several NMR structures, in which 10 unique nonterminal dinucleotide steps from the alternating AT sequences were analyzed.[62] In the ApT steps, the six-membered ring of the adenine is partially positioned over the thymine, while in the TpA step, the bases are relatively unstacked (Figure 5). This different stacking is reflected by the values of some helicoidal parameters (calculated using CURVES, with respect to the local helical axis) of the ApT and TpA steps. In particular, the differences are remarkable for the roll (−1.6 and 9.11°), slide (−1.2 and −1.6 Å), shift (−0.1 and 0.2 Å), and the twist (28.7 and 33.9°) parameters.

Coordination of Sodium Ions at the ApT Steps. The hydration is not only caused by water molecules but also by substantial contribution from the sodium ions. In our MD, the penetration of the sodium ions into the primary spine of

(62) Ulyanov, N. B.; James, T. L. *Methods Enzymol.* **1995**, *261*, 90−120.

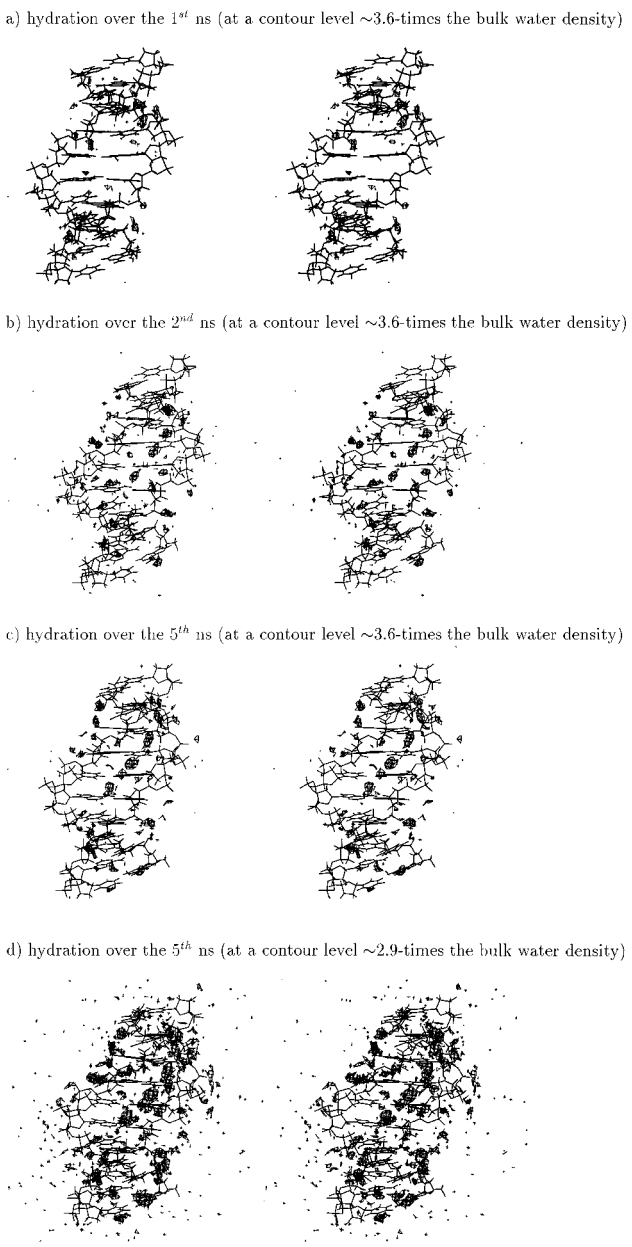

Figure 2. A stereoview picture of the averaged structures and their hydration (contoured water oxygen atom density) over the 1st (a), 2nd (b), and fifth (c) nanoseconds of the simulation starting from the canonical B-form of the $[d(AT)_5]_2$ decamer are presented. The contours of the water oxygen density at 1 ps intervals, into 0.5 Å^3 grid elements over a 50 Å^3 cubed grid, at a contour level of 15 hits per 0.5 Å^3 (~3.6-times the bulk water density) are displayed using the density delegate from MidasPlus.[61] The hydration over the fifth (d) nanosecond of the simulation starting from the canonical B-form of the $[d(AT)_5]_2$ decamer at lower density (a contour level of 12 hits per 0.5 Å^3 (~2.9-times the bulk water density)) is also depicted.

hydration is exclusively observed in the ApT steps. In accord with the nomenclature introduced by Young et al.,[21] we call these sites ApT pockets (the bottom of the minor groove at the ApT steps). The sodium ions are only coordinated in three ApT pockets (we call them "active ApT pockets") (Figure 6). No coordination of the sodium ions has been observed in the terminal ApT pockets. There are at least two reasons for such behavior. First, the terminal residues are too flexible, and second, the sodium ions coordinated in the terminal ApT pockets are not stabilized by a "two-side" negative potential as is the case for the middle pockets.

In the simulation starting from the canonical B-form of $[d(AT)_5]_2$, the coordination of the sodium ions was particularly observed in the first and the third active ApT pocket. The radial distribution function (RDF) calculated for this simulation (data not shown) reveals that the highest density of sodium ions is observed in the A3:T18-T4:A17 and the A7:T14-T8:A13 regions, which are the first and the third active ApT pockets. A sodium ion is localized in the first active ApT pocket. It adopted this position during the equilibration protocol, and it is quite strongly coordinated with O2s from T18 and T4 (the distances about 2.4 Å) atoms during the first nanosecond of the simulation. The strong coordination with the above-mentioned oxygen atoms and the strong repulsion between the sodium ion and each of the H2 hydrogens from adenines implies an extreme decrease of propeller twist into negative values. The average value of the propeller twist for the base pairs of this step, where the sodium ion was coordinated in the minor groove during the first nanosecond, is about −20°, while the remaining base pairs (except for the base pairs of the third active ApT pocket where another sodium ion was binded) exhibit values around −8°. The sodium ion interacts additionally with three water molecules in the minor groove. After about 1.1 ns, it moves away from the first active ApT pocket and is substituted by one of the neighboring water molecules. After this substitution, the sodium ion is coordinated in the secondary spine, where it remains for about 180 ps. After that, the ion is coordinated on the sugar−phosphate backbone for part of the time, and for the rest of the time, it is found further away from the DNA. After about 4 ns of the simulation, the sodium ion returns through the secondary spine into its original position in the first active ApT pocket. In this case, the process is very fast (Figure 7), and the ion stays in the original position until the end of the simulation. A similar situation occurs in the third active ApT pocket, the only difference being that there is no sodium ion localized in the primary spine at the beginning of the simulation. A sodium ion is localized in the secondary spine, and it is coordinated with a water molecule from the primary spine. After about 200 ps of the simulation, the sodium ion moves into the primary spine and becomes coordinated in the third active ApT pocket in the same way as the other sodium ion is coordinated in the first active ApT pocket. The sodium ion stays in the third active pocket for 1.6 ns, and then it moves away through the secondary spine (with the residence time of about 200 ps).

In the simulation starting from the canonical A-form, the coordination of sodium ions was observed in all active ApT pockets. A sodium ion was coordinated in the primary spine of the second active ApT pocket between 2.8 and 3.9 ns of the simulation. The first and the third active ApT pockets were symmetrically occupied by two sodium ions between the sixth and the seventh ns.

The above analysis has been focused on the first layer of hydration. However, the sodium ions are even more frequently seen in the second layer of hydration. In this case, they are coordinated with a water molecule from the first layer and the other five water molecules. Such a coordination is observed in the ApT and TpA steps, with a residence time of about 200 ps.

The Close Mutual Adenine Amino Group Contacts in the ApT Steps. It has already been noted that close mutual adenine N6−N6 contacts exist in the major groove of the ApT steps.[25,26] Since empirical potentials penalize the nonplanar geometries of the DNA base amino groups and underestimate the effect of the amino group nonplanarity on the intermolecular interaction energy,[63] we have to assume that formation of the close amino group contacts is likely to be underrepresented in our simula-

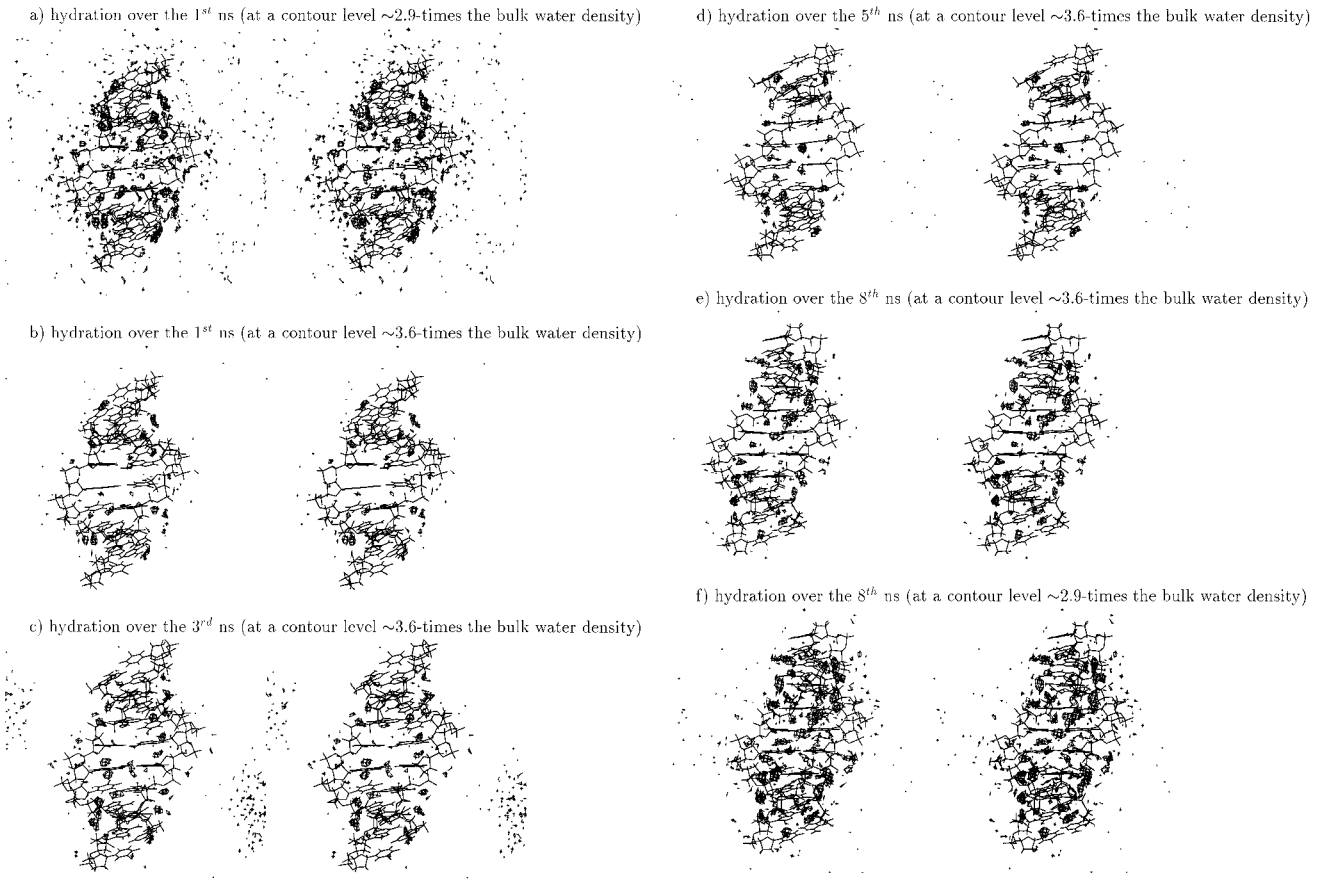

Figure 3. A stereoview picture of the averaged structures and their hydration (contoured water oxygen atom density) over the first (~2.9-times the bulk water density (a) and ~3.6-times the bulk water density (b)), third (~3.6-times the bulk water density (c)), fifth (~3.6-times the bulk water density (d)), and eighth (~3.6-times the bulk water density (e) and ~2.9-times the bulk water density (f)) nanoseconds of the simulation starting from the canonical A-form of the $[d(AT)_5]_2$ decamer are depicted. For more details see the text and Figure 2.

Figure 4. Two layers deep spine of hydration (~2.9-times the bulk water density) from MD.

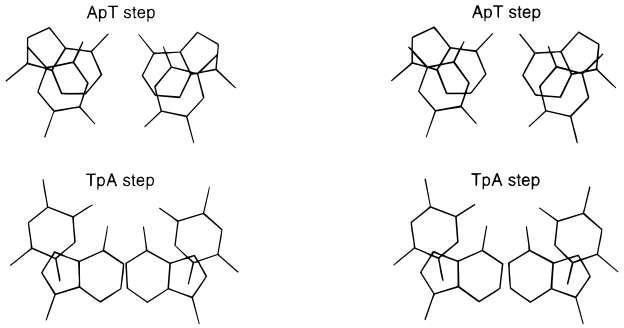

Figure 5. A stereoview of the average geometries of the ApT and TpA steps from MD simulations. Only the DNA bases (without hydrogen atoms) are depicted.

tions. In fact, no close amino group contacts were observed in the absence of sodium cations in the ApT pockets. In this case, the average N6−N6 distance in the ApT steps was about 3.6 Å in clear disagreement with the experimental values.[26] However, once the sodium ions became coordinated in the ApT pockets, the distance decreased to about 3.25 Å, which is very close to the average value from the high-resolution crystal structures (3.15 Å). On the basis of these data we propose that the sodium ions in the ApT pockets can stabilize the close mutual adenine amino group contacts in the ApT steps. This idea is supported by data shown in Figure 8 where the time course of interstrand

(63) Šponer, J.; Burcl, R.; Hobza, P. *J. Biomol. Struct. Dyn.* **1994**, *11*, 1357−1376.

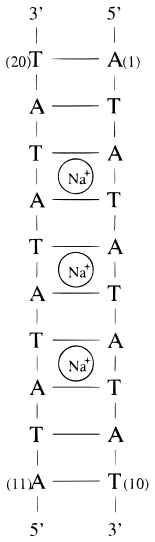

Figure 6. A schematic representation of the fractional occupancy by the sodium ions in the primary layers of the spine of hydration for the $[d(AT)_5]_2$ duplex structure. Only the [d(A3T4).d(A17T18)] (first active ApT pocket), [d(A5T6).d(A15T16)] (second active ApT pocket), and [d(A7T8).d(A13T14)] (third active ApT pocket) regions are occupied by the sodium ions in the primary spine.

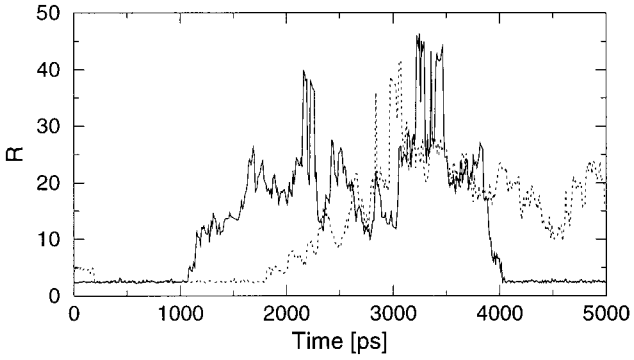

Figure 7. The distance *R* (Å) of a sodium ion from the O2(T18) atom (solid line) and the distance of another sodium ion from the O2(T8) atom (dotted line) as a function of time along the MD trajectory.

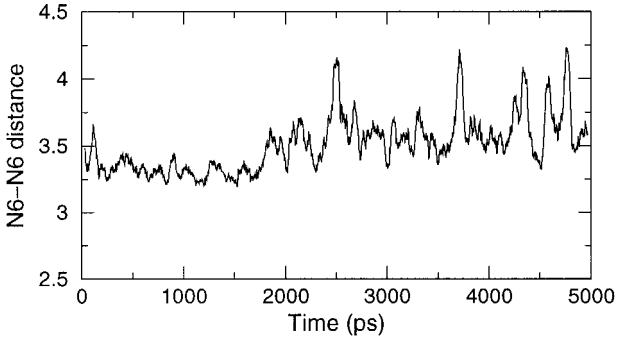

Figure 8. Time evolution of the interstrand amino group N6−N6 distances in the ApT step of the third active pocket. The data have been smoothed by performing a running average in time over 80 ps.

amino group N6−N6 distances is depicted. The situation reflects the behavior of the third active ApT pocket during the simulation starting from the canonical B-form of the $[d(AT)_5]_2$ decamer (vide supra). The N6−N6 distance during the period between 200 and 1800 ps, when the sodium ion is coordinated, is much more stable and shows smaller average values than during the rest of the simulation. Similar behavior was also observed for the other active ApT pockets, although the data is not shown

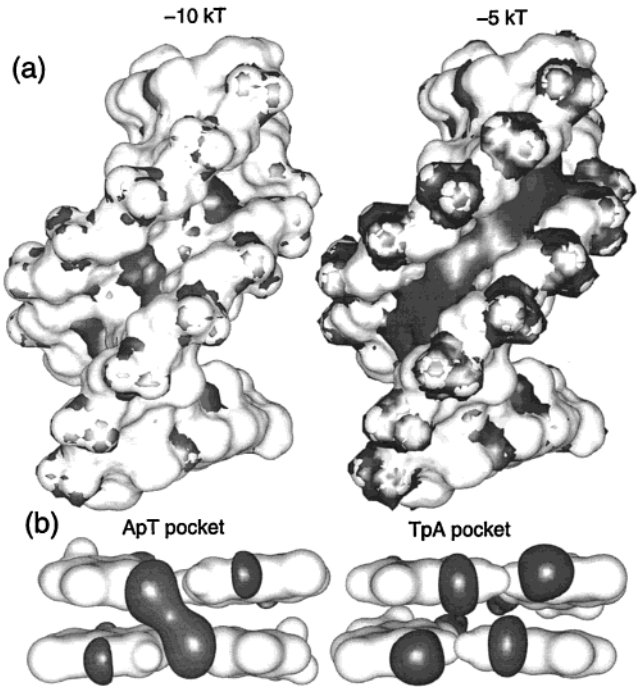

Figure 9. (a) The electrostatic potential calculated using the nonlinear Poisson−Boltzmann equation for the $[d(AT)_5]_2$ duplex is shown. The calculations were carried out using the DELPHI program. The −10 kT (left) and −5 kT (right) isopotential surfaces (in dark gray) with the DNA Connolly surface[78] (in white) are presented. The view is focused into the minor groove, where the "active ApT pockets" are clearly shown. (b) Calculated electrostatic potential of the ApT (left) and TpA (right) pockets represented only by DNA bases (the view into the minor groove). The density functional theory using the Becke 3LYP functional with the 6-31G** basis set was used. The calculations were performed using the TURBOMOLE program. Negative and positive isopotential surfaces are dark gray and white, respectively.

here. It is likely that these contacts are further stabilized by amino group pyramidalization effects[26] which we could not include with the present version of the force field.

Additional Analysis of Electrostatic Potentials of the ApT and TpA Pockets. To clarify whether ApT pockets are not preferred to bind sodium ions because of either the empirical potential used or the short duration of the trajectories on one hand or because of real physical nature on the other hand, we have performed two independent calculations, the first based on the nonlinear Poisson−Boltzmann equation and the second using the DFT method. Both calculations were carried out for the average structure from the last nanosecond of the simulation starting from the canonical B-form. The results are depicted in Figure 9a. The right part shows a strong negative potential spread on the bottom of the minor groove (−5 kT isopotential surface). Slightly lower negative potential (−10 kT isopotential surface) is especially spread in the ApT pockets. To summarize, the ApT pockets are clearly shown to concentrate lower electrostatic potential than the TpA pockets and, therefore, to attract cations.

The size and the distribution of the electrostatic potential of the ApT and TpA pockets calculated by the ab initio method are shown in Figure 9b. The lowest negative electrostatic potential is localized in four regions in the minor groove, near two O2 atoms and near two deprotonated N3 atoms. The protonated regions are associated with positive (repulsive) electrostatic potential. The uniquely low electrostatic potential of the ApT pocket is spread in the central part on the bottom of the minor groove.

Discussion

Our MD simulations of the $[d(AT)_5]_2$ decamer which started from different initial structures converged after about 500 ps to a common structure which exhibits the structural features of B-DNA. Similar convergence independent of the starting structures was also reported for the $[d(CCAACGTTGG)]_2$ duplex by Cheatham and Kollman[64,65] and for the $[d(CGCGAATTCGCG)]_2$ duplex by Cieplak et al.[66] However, none of the above works reports a "delay" in the convergence of the hydration patterns in comparison to the convergence of the oligonucleotide structure itself. We observed that the convergence of the hydration patterns requires a much longer time than the convergence of the oligonucleotide structure and also that it is strongly dependent on the starting geometry of the system. The equilibration protocol ensures that the water molecules are positioned in a different way at the beginning of the simulation for different starting geometries of the solute. In the case of the simulation starting from B-form, the solute does not principally change its conformation during the simulation and the stable hydration pattern (spine of hydration) is formed within 2−3 ns. However, once the hydration pattern is formed (or at least pre-formed), it takes a much longer time to reorganize it so that it fits a new conformation of the solute. This is seen in the simulation starting from A-form. While the A-to-B conformational change of the solute occurs within less than 1 ns, the spine of hydration needs another 5−7 ns to reorganize.

The spine of hydration is often discussed as a possible stabilizing effect of water on B-DNA. Macroscopic studies are fully consistent with this presumption showing a correlation between the change in entropy and the amount of bound water.[67] Nevertheless, seen from the microscopic point of view, the spine of hydration violates local B-canonicity. In other words, the local structure is different when the sodium ion is coordinated in the first layer in comparison with the local structure of the part where the water molecule is present in the first layer of hydration. This is not surprising as the sodium ion has completely different features from the water molecule. Since water molecules and sodium ions migrate quite frequently, the local structures also exhibit frequent changes which are dependent on what kind of spine molecule is present. The difference is particularly seen in the values of propeller twist (data not shown here).

The second issue addressed by this paper is the coordination of sodium ions. There are at least two key questions: where are the ions coordinated and what is the residence time. Recently, two theoretical works have been focused on the intrusion of sodium ions into the spine of hydration in the minor groove of B-DNA, both studying the dodecamer d(CGCGAATTCGCG).[21,22] The first report results from a 1.5 ns MD trajectory and additional PB calculations.[21] The authors observed a sodium ion coordinated in the ApT pocket during the first ∼500 ps, interacting favorably with two O2 thymine oxygens on the opposite strands of the duplex, and with oxygen atoms of four water molecules. They also showed by PB calculations that the minor groove AATT region is a favorable site for occupation by counterions. Finally, the authors presented a very valuable general scheme which suggests that favorable sites for occupation by counterions are in the major and minor groove between successive base pairs in a step and that the interaction sites are sequence-dependent and -specific. The second article[22] provides further data obtained by the extension of the original trajectory up to 5 ns. The new data shows further coordination of sodium ions at TpT (ApA) (with residence time ∼750 ps) and CpG (with residence time more than 1 ns) steps.

The important thing is that our results do not support the general hypothesis of sequence-specific pockets[21] and another hypothesis[68] which predicts cross-strand N3 adenine nitrogens in TpA steps (which have about the same distance as the cross-strand O2 thymine oxygens in the ApT steps, ∼4 Å) as a robust source of electronegative potential for a monovalent cation binding site. In our simulations, sodium ions were exclusively coordinated in the ApT steps. Our MD results are supported by data from high-resolution NMR spectroscopy[20] which shows that the cross-strand O2 thymine oxygens distance (∼4 Å) of the ApT step is relatively ideal for cation coordination, while the cross-strand O2 thymine oxygens distance (∼8 Å) of the TpA step is too long to participate directly in cation coordination. The reason the O2 thymine oxygen and the N3 adenine nitrogen play such different roles is that the N3 adenine nitrogen lone pair is probably much more conjugated with the adenine π-electron system than the O2 thymine oxygen lone pair is with the thymine π-system. This idea is also supported by Figure 9b, where the electrostatic potential contributions of individual atoms to the ApT and TpA pockets are depicted.

The experimental determination of the residence time of ions is dependent on the time scale accessible for the experimental method used. Processes on the millisecond time scale are quite easily reached.[69] Nevertheless, the residence time for the spine molecules is much shorter. The lower limit of the monovalent ions residence time has been estimated from NMR experiments to be at least 1 ns,[16] and the resident lifetime of waters in the spine of hydration is approximately 1 ns at 277 K.[16,70] Current MD simulations with explicit water are suitable for model processes up to 10 ns. It follows from our simulations that the residence time of sodium ions in the primary spine is between 1 and 2 ns. This time is somewhat longer than the residence time reported by Beveridge and co-workers for the d(CGCGAATTCGCG) dodecamer.[21,22] There are several examples in the literature showing that the additive potential used can bring a certain inaccuracy[71,72] especially describing interactions of charged particles (ions, protonated bases) or other strongly polar molecules with the DNA.[73,74] The reason is that the polarization is not explicitly included, due to the absence of the polarization term in the force field. The above authors suggest that the pairwise additive empirical potentials qualitatively underestimate the binding energy between the cation and the base.[74] If the above expectations are true, the residence times observed in MD simulations should be somewhat shorter than the real residence times. However, this question will remain open until we have accurate experimental data at hand. Such data could then be very useful for tuning empirical potentials.

(64) Cheatham, T. E., III; Kollman, P. A. *J. Mol. Biol.* **1996**, *259*, 434−444.
(65) Cheatham, T. E., III; Kollman, P. A. *J. Am. Chem. Soc.* **1997**, *119*, 4805−4825.
(66) Cieplak, P.; Cheatham, T. E., III; Kollman, P. A. *J. Am. Chem. Soc.* **1997**, *119*, 6722−6730.
(67) Rentzeperis, D.; Marky, L. A.; Kupke, D. W. *J. Phys. Chem.* **1992**, *96*, 9612.
(68) Bartenev, V. N.; Golovamov Eu, I.; Kapitonova, K. A.; Mokulskii, M. A.; Volkova, L. I.; Skuratovskii, I. *J. Mol. Biol.* **1983**, *169*, 217−234.
(69) Hud, N. V.; Schultze, P.; Sklenář, V.; Feigon, J. *J. Mol. Biol.* **1999**, *285*, 233−243.
(70) Maltseva, T. V.; Roselt, P.; Chattopadhyaya, J. *Nucleosides Nucleotides* **1998**, *17*, 1617−1634.
(71) Halgren, T. A. *Curr. Opin. Struct. Biol.* **1995**, *5*, 205−210.
(72) Šponer, J.; Gabb, H. A.; Leszczynski, J.; Hobza, P. *Biophys. J.* **1997**, *73*, 76−87.
(73) Šponer, J.; Leszczynski, J.; Vetterl, V.; Hobza, P. *J. Biomol. Struct. Dyn.* **1996**, *13*, 695−706.
(74) Šponer, J.; Burda, J. V.; Mejzlík, P.; Leszczynski, J.; Hobza, P. *J. Biomol. Struct. Dyn.* **1997**, *14*, 613−628.

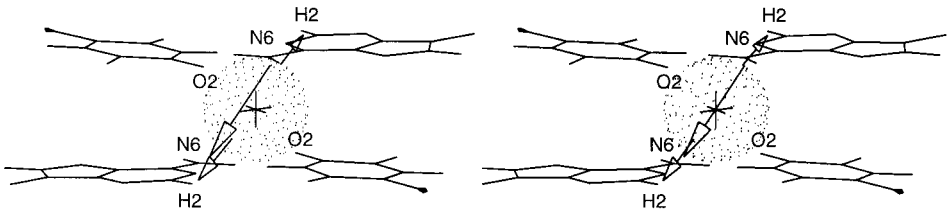

Figure 10. A stereoview picture of the [d(A3T4)].[d(A17T18)] region (first active ApT pocket). The structure is averaged over the first nanosecond of the simulation starting from the canonical B-DNA. A sodium ion and DNA bases of this step are displayed. An attractive interaction is between a sodium ion and two O2 thymine oxygen atoms (distances about 2.4 Å). The short arrows show a repulsive interaction between a sodium ion and two H2 adenine hydrogens. The long arrow shows the close N6−N6 mutual adenine amino group contact (3.25 Å). No minimization of this structure was performed and, therefore, some anomalous structural features, e.g., incorrect C−H lengths in methyl groups, are present.

As pointed out above, the coordination of sodium ions strongly enhances the propeller twist. Since values of propeller twist in crystal structures are assumed not to be influenced by crystal packing or lattice forces[75] and since all of the above data show that sodium ions are, at least temporarily, a part of the spine of hydration, we should see two peaks when plotting values of the propeller twist for the ApT steps from structures found in the crystallographic database. However, we were not successful in this, as we obtained a wide and fuzzy distribution of the propeller twist. One of the reasons could be that experimental errors in the propeller twist of most deposited crystal structures are sufficiently high, as was discussed by Williams and co-workers.[13] Another reason could be too short a time scale within which the sodium ions exchange. But this is less probable because of the residence times mentioned above. The third possible reason is that the experimental data mirrors a dynamic equilibrium of two possible states.

The third issue addressed by this paper is that of the close mutual adenine amino group contacts observed in almost all ApT B-DNA steps in oligonucleotide crystal structures. They have been rationalized, on the basis of quantum chemical calculations, as a consequence of the high flexibility of amino groups leading to a nonsymmetric arrangement of two amino groups in which one group acts as donor and the other as an acceptor.[26,27] Since the currently used force field does not properly account for the amino group pyramidalization effects, we assumed that such contacts will not be formed in the course of our simulations.[63] Indeed, for a rather large fraction of the simulation time we saw no N6−N6 amino group contacts. Nevertheless, we have observed in our simulation that the interatomic distance between N6 adenine nitrogens decreases substantially when a sodium ion is coordinated in the ApT pocket. This observation can be rationalized by a simple mechanistic hypothesis suggested in Figure 10. The sodium ion is directly coordinated by the O2 thymine oxygen atoms and, simultaneously, repulses the adjacent H2 adenine hydrogen atoms. This repulsive effect on the hydrogen atoms in the minor groove causes a counter-rotation of adenine bases in such a way that the amino groups in the major groove are contacted.

The above observation leads us to a hypothesis suggesting a relationship between the coordination of sodium ions at the ApT steps and the close mutual adenine amino group contacts. To verify this hypothesis we have examined the NDB database. We took 12 oligonucleotide crystal structures with the best resolution (≤1.7 Å, summarized in Table 1) and divided them into dinucleotide steps (the terminal steps were omitted because of end effects). The dinucleotide steps were subjected to RMSD analysis, which unambiguously showed the highly conserved geometry of the ApT steps which were locked in geometries with a large propeller twist and close N6−N6 contacts. We propose that both the amino group close contacts in the major groove and the coordinated sodium ions in the minor groove contribute simultaneously to this "stability" of the ApT steps. It is seen in Table 1 that the ApA steps also show a high similarity, which is probably a consequence of the three-center hydrogen bond.[76,77]

Table 1. RMSD Analysis of Dinucleotide Steps from the Oligonucleotide Crystal Structures[a]

step	number of steps included	RMSD and SD
ApT	12	0.24 ± 0.11 Å
ApA	12	0.28 ± 0.16 Å
CpG	13	0.36 ± 0.19 Å
GpA	13	0.39 ± 0.23 Å
TpA	3	0.55 ± 0.05 Å

[a] Only the high-resolution crystal structures were analyzed, NDB codes: BD0005 (*R* 1.5 Å), BD0012 (*R* 1.2 Å), BD0016 (*R* 0.9 Å), BD0018 (*R* 1.3 Å), BD0019 (*R* 1.7 Å), BDJ017 (*R* 1.6 Å), BDJ019 (*R* 1.4 Å), BDJ025 (*R* 1.5 Å), BDJ031 (*R* 1.5 Å), BDJ036 (*R* 1.7 Å), BDJ060 (*R* 1.7 Å), BDL084 (*R* 1.4 Å).

Acknowledgment. We would like to thank Dr. Jaroslav Kypr (Institute of Biophysics AVČR, Brno) for critical reading of the manuscript and comments. R.Š. also thanks Nada Špačková (IB AVČR, Brno) for helpful discussions. The authors are grateful to Dr. Juli Feigon and co-workers (UCLA) for providing an advance copy of a valued manuscript and Mr. Laurence Benjamin, B.A. for language corrections. The authors also thank the reviewers for valuable comments. The research presented here has partially been supported by The Ministry of Education of The Czech Republic, Grant No. VS 96095. The Academic Supercomputer Center in Brno and Prague are acknowledged for providing authors with access to computer facilities. This paper is dedicated to Professor Milan Kratochvíl on the occasion of his 75th birthday.

JA9912170

(75) Dickerson, R. E.; Goodsell, D. S.; Neidle, S. A. *Proc. Natl. Acad. Sci. U.S.A.* **1994**, *91*, 3579−3583.

(76) Nelson, H. C.; Finch, J. T.; Luisi, B. F.; Klug, A. *Nature* **1987**, *330*, 221−226.

(77) Yanagi, K.; Prive, G. G.; Dickerson, R. E. *J. Mol. Biol.* **1991**, *217*, 201−214.

(78) Connolly, M. L. *Science* **1983**, *221*, 709−713.